THE JOURNAL OF BIOLOGICAL CHEMISTRY
Vol. 271, No. 31, Issue of August 2, pp. 18743–18748, 1996

Printed in U.S.A.

EPR and Mössbauer Spectroscopic Studies on Enoate Reductase*

(Received for publication, January 26, 1996, and in revised form, March 26, 1996)

Jorge Caldeira‡§, Richard Feicht¶, Hiltturd White¶, Miguel Teixeira‡‖, José J. G. Moura‡, Helmut Simon¶, and Isabel Moura‡**

From the ‡Departamento de Química (and Centro de Química Fina e Biotecnologia), Faculdade de Ciências e Tecnologia, Universidade Nova de Lisboa, 2825 Monte de Caparica, Portugal, the §Instituto Superior de Ciências da Saúde Sul, 2825 Monte de Caparica, Portugal, the ¶Lehrstuhl für Organische Chemie und Biochemie, Technischen Universität München, D-85747 Garching, Germany, and the ‖Instituto de Tecnologia Química e Biologica, Universidade Nova de Lisboa, Apt. 127, 2780 Oeiras, Portugal

Enoate reductase (EC 1.3.1.31) is a protein isolated from *Clostridium tyrobutyricum* that contains iron, labile sulfide, FAD, and FMN. The enzyme reduces the α,β carbon-carbon double bond of nonactivated 2-enoates and in a reversible way that of 2-enals at the expense of NADH or reduced methyl viologen. UV-visible and EPR potentiometric titrations detect a semiquinone species in redox intermediate states characterized by an isotropic EPR signal at $g = 2.0$ without contribution at 580 nm. EPR redox titration shows two widely spread mid-point redox potentials (−190 and −350 mV at pH 7.0), and a nearly stoichiometric amount of this species is detected. The data suggest the semiquinone radical has an anionic nature. In the reduced form, the [Fe-S] moiety is characterized by a single rhombic EPR spectrum, observed in a wide range of temperatures (4.2–60 K) with g values at 2.013, 1.943, and 1.860 (−180 mV at pH 7.0). The g_{max} value is low when compared with what has been reported for other iron-sulfur clusters. Mössbauer studies reveal the presence of a $[4Fe\text{-}4S]^{+2/+1}$ center. One of the subcomponents of the spectrum shows an unusually large value of quadrupole splitting (ferrous character) in both the oxidized and reduced states. Substrate binding to the reduced enzyme induces subtle changes in the spectroscopic Mössbauer parameters. The Mössbauer data together with known kinetic information suggest the involvement of this iron-sulfur center in the enzyme mechanism.

Enoate reductase (EC 1.3.1.31) (1–6) isolated from *Clostridium tyrobutyricum* catalyzes the NADH or methyl-viologen-dependent reduction of the α,β carbon-carbon double bond of nonactivated 2-enoates (7) and in a reversible way that of 2-enals (8). The enzyme appears to be a multimer of identical subunits. The total molecular mass is 940 kDa (subunit circa 73 kDa). Sedimentation equilibrium experiments, molecular mass data, and electron microscopy indicate that the native enzyme is composed of a tetramer of trimers. Per enzyme subunit 1 FAD, 0.6 FMN, 4 iron, and 4 labile sulfur atoms were found (9), and thus enoate reductase belongs to the rare class of flavoenzymes containing both FAD and FMN. The involvement of iron-sulfur centers in electron transfer is well established (10), and they have also been shown to be associated with other important physiological nonredox functions, such as those of aconitase and other dehydratases (11, 12), glutamine 5-phosphoribosyl-1-pyrophosphate aminotransferase (13), endonuclease III (14), and iron-responsive element-binding protein (15–17).

In this work, we report the involvement of an iron-sulfur center in a new type of biochemical reaction. EPR and Mössbauer data are analyzed in the oxidized and NADH- and dithionite-reduced states, as well as in substrate bound forms in order to identify the type of iron-sulfur core involved. A tentative mechanism is presented that involves a hydride transfer from a flavin group and a carbon-carbon double bond polarized by the presence of the iron-sulfur cluster, thus including enoate reductase in the group of iron-sulfur enzymes in which the metal center interacts with substrate molecules during catalysis.

MATERIALS AND METHODS

Growth of C. tyrobutyricum (DSM 1460)—Cells of *C. tyrobutyricum* DSM1460 were grown on ^{57}Fe- or ^{56}Fe-containing medium on a 50-liter scale according to Bader and co-workers (1) with slight modifications (1–3). The medium contained 150 mg/liter $(NH_4)_3SO_4$ instead of $(NH_4)_2PO_4$ and additionally 32 mg $Na_2SO_4 \cdot 10\ H_2O$. The source of iron was about 65 mg of ^{57}Fe in the form of an $^{57}FeSO_4$ solution, *i.e.*, the concentration amounted to about 2×10^{-5} M iron. The cells were harvested by centrifugation after reaching the stationary phase 20 h after inoculation.

Purification and Sample Preparation—Enoate reductase was purified under strict anaerobic conditions essentially according to Kuno *et al.* (9). Wet packed cells (78 g) were suspended in 234 ml of 50 mM potassium phosphate buffer, pH 7.0, containing 10 mM sodium tiglate, 1 mM EDTA, 320 mg of lysozyme, and 32 mg of DNase. The pH of the suspension was adjusted to 7.2 by the addition of 2.5 M Na_2CO_3. After incubating the suspension for 40 min at 35 °C, it was centrifuged for 20 min at 27000 × *g* at 0 °C. The careful control of the pH is crucial for obtaining the enoate reductase in the supernatant.

All chromatographic steps were performed with oxygen-free buffers containing 0.1 mM EDTA, 250 mM saccharose, 0.02% sodium azide, and 0.02% mercaptoethanol. The supernatant was applied to the following columns in two portions.

It was first applied to a DEAE Sepharose CL-6B column (18.5 × 4.5 cm) equilibrated with 20 mM potassium phosphate buffer (pH 7.0) and then applied directly to a hydroxyapatite column (18 × 2.4 cm) as described previously (3).

Pure enoate reductase both in ^{57}Fe and in ^{56}Fe were concentrated in phosphate buffer, pH 7.0, 0.25 M saccharose, and 1 mM crotonate (needed to maintain the enzyme in the oxidized state). In the final steps the enzyme buffer was exchanged with a buffer containing only phosphate and saccharose in the concentrations mentioned above. Enoate reductase in ^{57}Fe at the final concentration of about 1 mM was used to prepare four samples: native, dithionite-reduced, NADH-reduced, and dithionite-reduced in the presence of 50 mM of cinnamate. The enzyme reductions were performed under strict anaerobic conditions.

Spectroscopic/Potentiometric Measurements—Redox potentials of enoate reductase were determined by UV-visible absorbance and EPR potentiometric titrations. The protein solution in phosphate buffer, pH 7.0, was kept under anaerobic conditions by flushing the solution during the titration with purified Argon (with an Indicating Oxygen Trap from Chemical Research Supplies). An optical redox cell and an EPR

* The costs of publication of this article were defrayed in part by the payment of page charges. This article must therefore be hereby marked "*advertisement*" in accordance with 18 U.S.C. Section 1734 solely to indicate this fact.

** To whom correspondence should be addressed. Tel.: 351-1-2948381; Fax: 351-1-2948550; E-mail: isa@dq.fct.unl.pt.

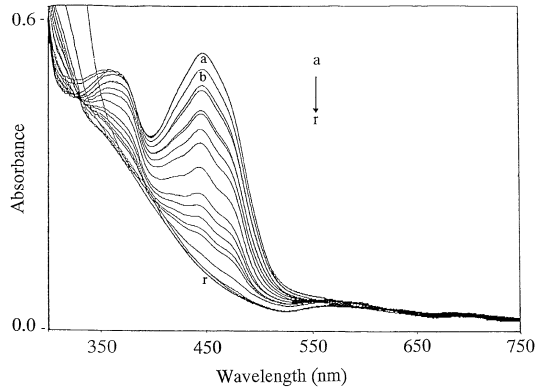

FIG. 1. **UV-visible spectra of enoate reductase at different redox potentials.** Spectra were obtained with a protein concentration of 17 μM in phosphate buffer 0.7 M with pH 7.0. at the following poised redox potentials: *a*, +54; *b*, +49; *c*, +42; *d*, +36; *e*, -22; *f*, −48; *g*, −105; *h*, −123; *I*, −140; *j*, −147; *k*, −155; *l*, −167; *m*, −180; *n*, −191; *o*, −198 *p*, −275; *q*, −291; *r*, −338 mV.

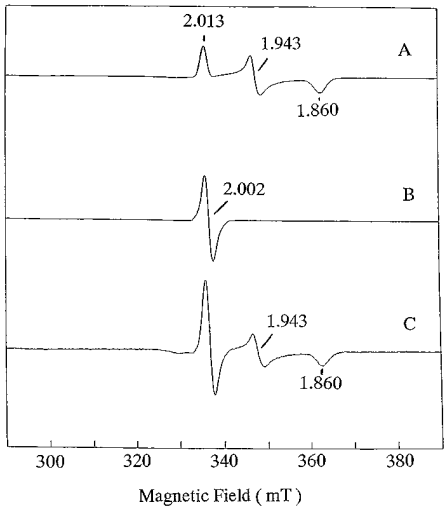

FIG. 2. **EPR spectra of enoate reductase reduced with dithionite measured at 10 K (*A*) and sample reduced with NADH recorded at 120 (*B*) and 10 K (*C*).** Other experimental conditions are: microwave frequency, 9.43 GHz; microwave power, 23.5 μW, modulation amplitude, 1 millitesla; modulation frequency, 100 KHz; receiver gain, 5×10^4; protein concentration, 96 μM.

potentiometric cell, slightly modified from the design of Dutton (18) was used for the UV-visible and EPR titrations. The potentials were measured with a Crison 2002 potentiometer with a platinum and a Ag/AgCl electrode and are quoted relative to the normal standard hydrogen electrode and calibrated with quinhydrone at pH 7.0. The following redox mediators were present at a final concentration of 3.5 μM: 1,4-naphtoquinone, methylene blue, triquat, phenosaphranine, benzylviologen, methylviologen, dichlorophenol-indophenol, benzoquinone, anthraquinone-2-sulfonic acid, phenazinamethosulfate, dimethyltriquat, indigo tetrasulfonate, 2-hydroxy-1,4-naphtoquinone, 5-hydroxy-1,4-naphtoquinone, duroquinone, phenazil, and safranine.

Solution potentials were varied by adding appropriate volumes of deareated 30 mM sodium dithionite or 30 mM NADH as reductant. UV-visible spectra were recorded during titration on a UV-265FS Shimadzu spectrometer. EPR redox titrations were performed in the same conditions as described for the UV-visible titrations, and the potentials were varied as described in Ref. 9. The protein solution was poised at different redox potentials, and 180-μl aliquots were transferred under argon to EPR tubes and frozen in liquid nitrogen for later measurement.

EPR spectra were made on a Bruker ER 200 spectrometer equipped with an Oxford continuous flow cryostat. The Mössbauer spectrometer was similar to the one described in Ref. 19. The zero velocity of the Mössbauer spectra is referred to the centroid of metallic iron spectra at room temperature.

RESULTS

UV-visible and EPR Redox Titrations

The UV-visible spectra of enoate reductase are largely dominated by the flavin cofactor in the 300–550 nm region. UV-visible measurements coupled with potentiometric titrations as shown in Fig. 1 do not distinguish between the flavin and [Fe-S] absorbance contribution due to the similarity of the redox potentials of these prosthetic groups. Also no 580–600 nm spectral contribution was detected in the UV-visible spectrum during redox titrations. The native form of enoate reductase is EPR silent, and the iron-sulfur and the flavin moieties are both diamagnetic (not shown).

At 10 K, the EPR spectrum of the NADH-reduced state shows a rhombic signal with *g* values at 2.013, 1.943, and 1.860, which are assigned to an iron-sulfur center with a superimposed isotropic signal centered at $g = 2.00$, attributable to a flavin semiquinone (see Fig. 2*C*). At high temperature (120 K), the iron-sulfur center is too broad to be detected, and the EPR features are dominated by the flavin radical signal (Fig. 2*B*). The dithionite-reduced enzyme shows the same rhombic EPR signal as the NADH-reduced sample, but the isotropic signal is absent (Fig. 2*A*). The intensity of the rhombic EPR signals does not increase upon further reduction with dithionite: the spin quantification (relative to a CuEDTA standard) gives 0.94 spin per monomer. The quantitation of the flavin signal is 0.9 spin per monomer, using as a standard *Desulfovibrio desulfuricans* ATCC 27774 flavodoxin in the semiquinone state at 120 K (20). The temperature dependence of the rhombic signal shows that it can be detected up to 60 K and is better observed at 10 K, using a microwave power of 23.7 μW. The line width of this rhombic species is increased in the ^{57}Fe-enriched sample due to unresolved hyperfine interactions.

The optimal temperature to observe the isotropic signal attributable to the flavin is 120 K. A comparison of the EPR signals of the flavin radical in H_2O and D_2O shows a line width reduction from 17 to 13 G (21). This observation is not in agreement with what was previously reported for anionic semiquinones where a decrease in the line width from 15 to 14 G was found, whereas in the neutral semiquinones the line width changes from 19 to 15 G due to the permutation of the flavin N-5 exchangeable proton. The span in redox potentials for this redox equilibrium (see below) is large enough ($\Delta = 170$ mV) to generate a nearly stoichiometric amount of the intermediate redox form. Then, in conclusion, despite the anomalous line width behavior, an anionic semiquinone form is present in this enzyme. Fig. 3 shows the relative intensity of the EPR spectrum of the [FeS] center recorded at 10 K *versus* the poised redox potential. The experimental data were fitted with a monoelectronic Nernst curve with a midpoint redox potential of −180 mV when dithionite is used as the reducing agent. When the protein is titrated with NADH, the midpoint potential was found to be −167 mV (error bar ± 15 mV). The relative intensity of the semiquinone EPR spectrum recorded at 120 K follows a bell shaped curve, which was fitted using a simple sequential redox model (see Fig. 3) and assuming a maximum intensity of 0.9 spin, and the mid-point redox potentials determined were −190/−177 mV for the quinone/semiquinone couple (using either dithionite or NADH as reducing agent) and −350 mV for the semiquinone/hydroquinone couple (using dithionite). The redox titration performed in the presence of NADH, does not reach a redox potential value below −300 mV.

Mössbauer Spectroscopy

Oxidized State

High Temperature Spectra—The Mössbauer spectra of the native enzyme enriched in ^{57}Fe were recorded at 80, 100, and 130 K.

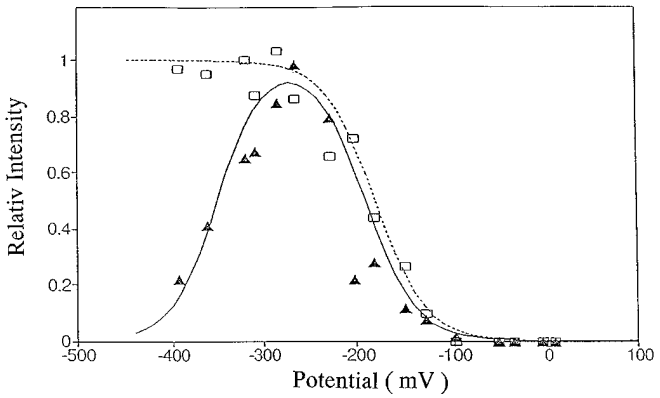

FIG. 3. **Relative intensity of the flavin (△) and FeS center (□) EPR signals as function of measured redox potential (*versus* normal hydrogen electrode).** *Solid* and *dashed lines* correspond to the Nernst fit to the flavin and FeS center, respectively, using redox potentials given in the text.

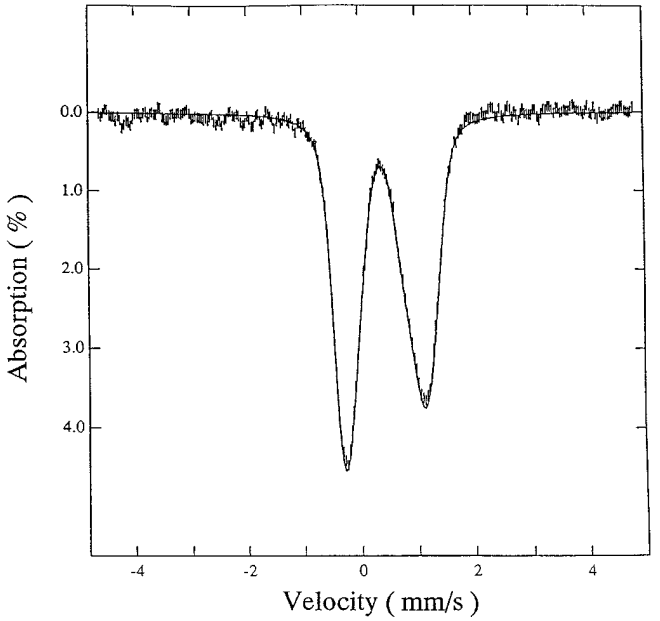

FIG. 4. **Mössbauer spectrum of native enoate reductase recorded at 130 K.** The *solid line* corresponds to the least square fitting of quadrupole doublets to the spectrum.

Fig. 4 shows the spectrum obtained at 130 K. An asymmetric quadrupole doublet is observed with different line widths for the positive velocity peak and the negative velocity peak.

The high temperature spectrum was fitted with subcomponents that have an average isomer shift (δ) of 0.43 mm/s and an average quadrupole splitting (ΔE_Q) varying from 1.30 to 1.33 mm/s depending on the recording temperature. These Mössbauer parameters are characteristic of high spin iron in an oxidation state intermediate between the ferric and ferrous states, suggesting electron delocalization and tetrahedral coordinated by weak field ligands, such as sulfur atoms.

The analysis of these parameters and the temperature dependence of the quadrupole splitting (not shown) indicate that this cluster has some ferrous character in the native state, excluding the possibility of the presence of an oxidized [2Fe-2S] cluster, which contains only ferric atoms.

Low Temperature Spectra—The Mössbauer spectra of the protein as isolated were recorded at 4.2 K in the presence of an applied magnetic field of 0.0, 4.0 or 8.0 tesla (Fig. 5). The spectra were simulated with four subcomponents, using an S = 0 spin Hamiltonian. The simulated spectra are shown as the

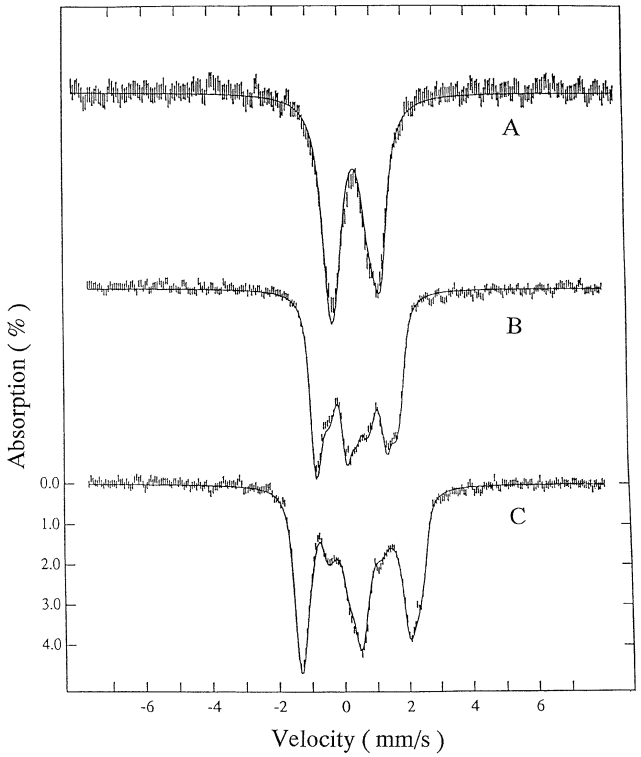

FIG. 5. **Mössbauer spectra of native enoate reductase [4Fe-4S]$^{2+}$ cluster recorded at 4.2 K.** The spectra were recorded with an applied magnetic field of 0.0 (*A*), 4.0 (*B*), and 8.0 tesla (*C*), parallel to the γ beam. The *solid lines* plotted over the experimental spectra represent the theoretical simulation of the [4Fe-4S]$^{2+}$ cluster, with the parameters reported in the text.

solid lines in Fig. 5, with the parameters summarized in Table I. The good agreement between the theoretical and experimental data indicates that all the iron atoms in the sample are in a diamagnetic environment in agreement with the EPR results. The diamagnetism of the center results from the antiferromagnetic coupling of the *d* electrons of the two ferric and two ferrous high spin iron atoms. The parameters shown in Table I are characteristic of a [4Fe-4S]$^{+2}$ cluster, but the mean value of the quadrupole splitting, and in particular the mean value of the isomer shift, is high when compared with reported values for this class of cluster.

Reduced State

High Temperature Spectra—The Mössbauer spectrum of the dithionite-reduced sample observed at high temperature (100 K) shows two resolved quadrupole doublets corresponding to the mixed valence and ferrous pairs (Fig. 6). In the ferrous pair, a small nonequivalence (*broader line*) is noticed in the peak detected at positive velocity. However, a deconvolution of these two subsites was not attempted due to the poor spectral resolution. For this reason, the data were fitted with two quadrupole doublets in a 1:1 ratio. The mixed valence pair has ΔE_Q = 1.22 mm/s and δ = 0.50 mm/s. The ferrous pair in the dithionite-reduced sample has ΔE_Q = 2.32 mm/s and δ = 0.61(4) mm/s. This value of quadrupole splitting is the highest reported for a [4Fe-4S]$^{+1}$ center in biological systems (see Table II).

Low Temperature Spectra—The Mössbauer spectra recorded at 4.2 K with applied magnetic fields of 0.095, 4.0, and 8.0 tesla are characteristic of a paramagnetic species with an S = 1/2 spin system (Fig. 7). The experimental data were fitted with an S = 1/2 spin Hamiltonian:

TABLE I
Mössbauer simulation parameters of the oxidized sample at 4.2 K (average ΔE_Q and δ values are 1.359 and 0.4615 mm/s, respectively)

Site	ΔE_Q	δ	Γ	η
		mm/s		
I	1.63	0.49	0.29	0.40
II	1.62	0.49	0.29	0.45
III	1.29	0.45	0.30	0.7
IV	0.90	0.41	0.29	1.89

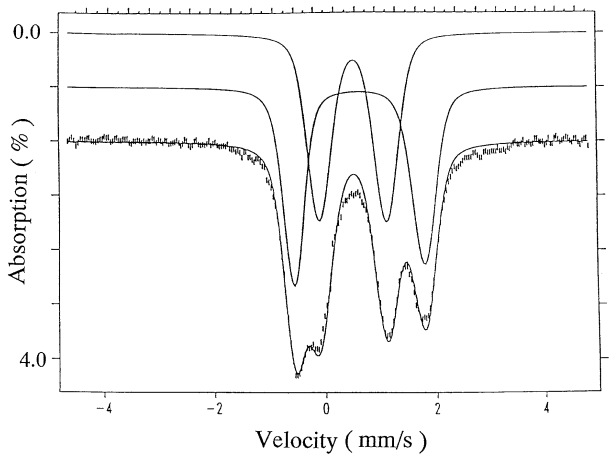

FIG. 6. **Mössbauer spectrum of dithionite-reduced enoate reductase recorded at 100 K.** The *solid line* plotted over the experimental spectrum is a least square fit of two quadrupole doublets to the spectrum (*solid lines* plotted above).

TABLE II
Mössbauer simulation parameters of enoate reductase at 100 K, reduced with dithionite, NADH and by dithionite in the presence of 50 mM of cinnamate

Sample	ΔE_Q	δ
	mm/s	
Dithionite-reduced	2.32	0.61
	1.22	0.50
NADH-reduced	2.34	0.61
	1.20	0.49
Dithionite-reduced in the presence of cinnamate	2.31	0.61
	1.20	0.48

$$\hat{H} = \beta_e \vec{S} \cdot \tilde{g}_e \cdot \vec{H} + \vec{S} \cdot \tilde{A} \cdot \vec{I} + \frac{eQV}{4}\left[I_z^2 - \frac{I(L+1)}{3} + \frac{\eta}{3}(I_x^2 - I_y^2)\right] - \tilde{g}_n \beta_n \vec{H} \cdot \vec{I}$$

using the WMOSS analysis program from WEB Research Co. (Edina, MN). Two major sites were identified by the inner and outer movement of the spectral lines when the externally applied magnetic field is increased, corresponding to negative or positive hyperfine coupling constants (22). The site with positive coupling constants (ferrous component) was subdivided for analysis proposes into two subsites (a and b). The sites with negative coupling constants were labeled 2c. This model was adopted to improve the simulation, taking into account small nonequivalence among sites (already detected in the high temperature spectra). The subsite differentiation is more evident when small spectral changes are analyzed on cluster data obtained in the presence or the absence of substrate (see below).

The parameters used in the data analysis of the reduced samples are presented in Table III. The ΔE_Q value for the ferrous pair in this cluster is higher than commonly found in ferredoxin type clusters. Site 2c has δ = 0.53 mm/s and ΔE_Q = 1.34 mm/s and negative hyperfine coupling constants (−23.2, −28.4, and −24.0 tesla) and was therefore identified as the mixed valence (ferric/ferrous) pair. The ferrous site *a* has ΔE_Q = +2.4 mm/s and δ = 0.65 mm/s, whereas ferrous site *b* has

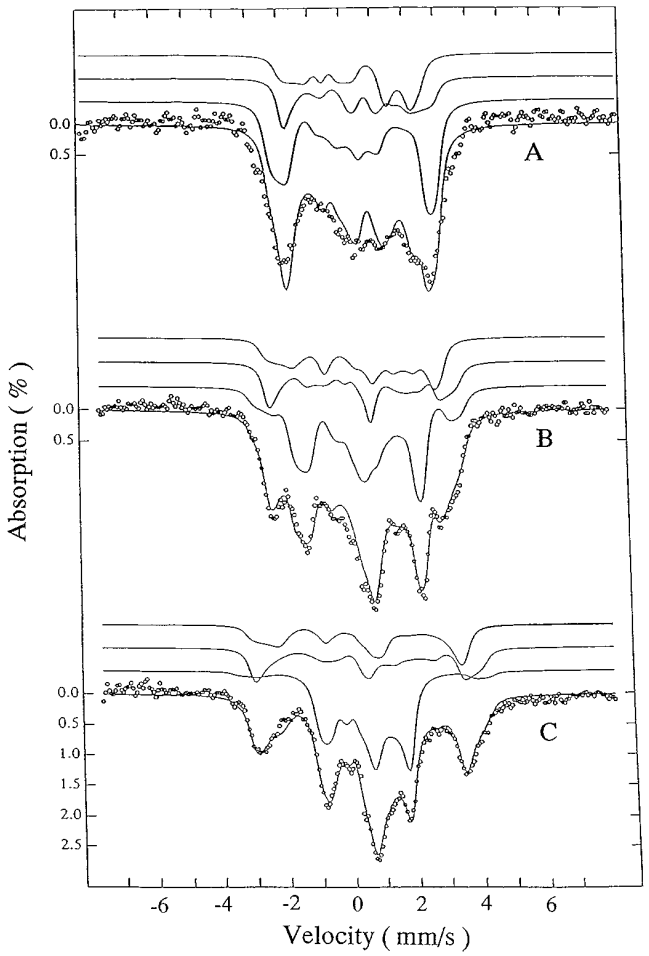

FIG. 7. **Mössbauer spectra of dithionite-reduced [4Fe-4S]$^{1+}$ cluster recorded at 4.2 K.** The spectra were recorded with a magnetic field of 0.095 (*A*), 4.0 (*B*), and 8.0 tesla (*C*) applied parallel to the γ radiation. The *solid lines* above the spectra represent the components of the theoretical simulation according to the text, and the *solid line* over the spectra represents the sum of simulation components.

ΔE_Q = -2.39 mm/s and δ = 0.61 mm/s.

Analysis of the Hyperfine Parameters—The simulation of the low temperature spectra recorded in the presence of strong externally applied magnetic fields allow determination of the values of the ^{57}Fe hyperfine coupling constants (Fig. 7). The average value of the splitting constants of the mixed valence pair is found to be similar in most of the analyzed [4Fe-4S] clusters and ranges from −17 to −26 tesla. Somewhat higher variability is found in the average splittings of the ferrous pair, which range from +3 to +15 tesla. The intrinsic value of the coupling constant in a iron ion coordinated by an oxygen atom is higher than that with a sulfur ligand. However, as it has been shown (23–25), the magnitude of A is also dependent on the spin projection, and this parameter cannot be taken as absolutely conclusive of oxygen coordination. Fig. 8 shows the average values of the hyperfine coupling constant of the ferrous and ferric components in iron-sulfur clusters. Enoate reductase shows the second highest hyperfine coupling constants after aconitase.

Interaction of Reduced Enoate Reductase with Substrate—Modifications were observed in the Mössbauer spectra of the reduced protein in the presence of substrate (Fig. 9). The peak at −3.8 mm/s in the 8 tesla spectrum is sharper in the presence of substrates while some other minor modifications occur in other parts of the spectra (compare Figs. 7 and 9). A simulation of this spectrum was done and required some adjustments in

TABLE III
Mössbauer fitting parameters of reduced samples at 4.2 K with an applied magnetic field of 0.095, 4.0, and 8.0 tesla

	Site	ΔE_Q	δ	$A_{xx}/g_n\beta_n$	$A_{yy}/g_n/\beta_n$	$A_{zz}/g_n\beta_n$	η
		mm/s			*Tesla*		
Reduced with dithionite	Fe_a	+2.39 (7)	0.64 (5)	6.7	20.5	4.2	0.0
	Fe_b	−2.38 (6)	0.61 (4)	5.6	23.4	16.2	−1.0
	Fe_{2c}	+1.42 (3)	0.53 (3)	−23.2	−28.4	−24.0	0.8
Reduced with NADH	Fe_a	+2.39 (6)	0.59 (3)	3.1	21.9	7.2	0.2
	Fe_b	−2.41 (8)	0.59 (1)	4.5	23.4	15.2	−0.8
	Fe_{2c}	1.39 (5)	0.55 (0)	−22.7	−29.0	−24.5	0.9
Reduced with dithionite and cinnamate	Fe_a	2.39 (5)	0.59 (3)	3.6	21.1	7.2	0.2
	Fe_b	−2.47 (9)	0.59 (1)	5.3	21.7	14.7	−0.8
	Fe_{2c}	1.39 (6)	0.55 (0)	−24.6	−30.0	−23.9	0.6

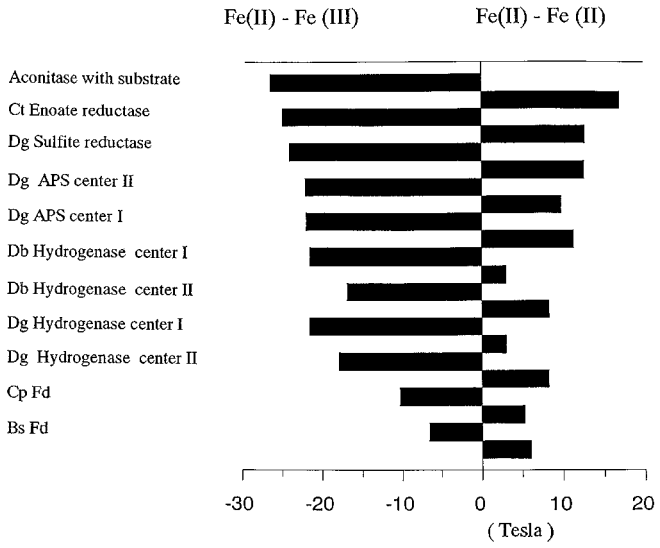

FIG. 8. **Comparison of the average hyperfine coupling constants of [4Fe-4S]$^{1+}$ clusters.** The plotted data are the reported averages of the *x*, *y*, and *z* hyperfine coupling constants of the mixed valence pairs and ferrous pairs of the [4Fe-4S]$^{1+}$ clusters.

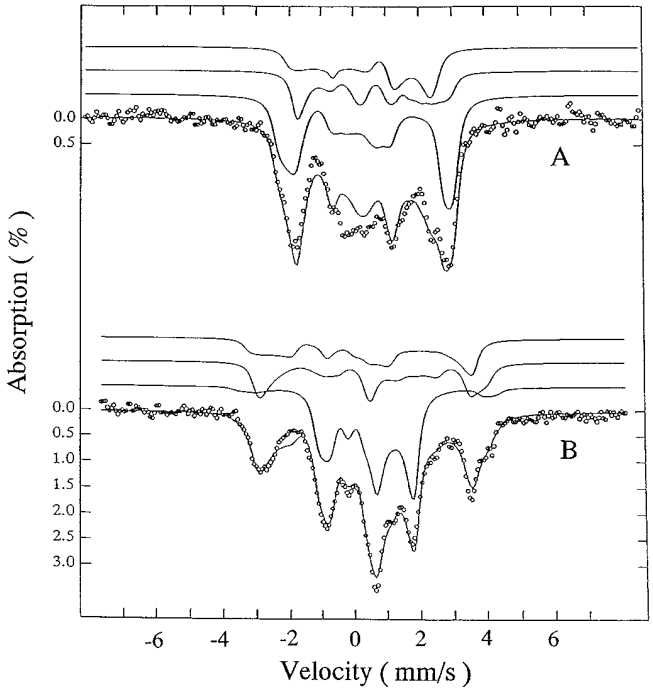

FIG. 9. **Mössbauer spectra of dithionite-reduced enoate reductase in the presence of cinnamate recorded at 4.2 K.** The spectra were recorded with a magnetic field of 0.095 (*A*) and 8.0 tesla (*B*) applied parallel to the γ radiation. The *solid lines* above the spectra represent the components of the theoretical simulation according to the text, and the *solid line* over the spectra represents the overall simulation.

the overall set of parameters as indicated in Table III. This table also presents the parameters used for the fitting of the Mössbauer spectra of the NADH-reduced sample. The changes are small and reflect subtle differences in the chemical environment of the cluster.

DISCUSSION

Comparison of 4.2 K Mössbauer Parameters of the +1 and +2 Oxidation States—Iron-sulfur centers show a wide structural variability in terms of metal stoichiometry and coordination. They may contain from one to six iron atoms, and the metal core can have only sulfur coordination, but other ligands can also be present substituting for cysteinyl residues. [2Fe-2S] clusters can have nitrogen containing ligands (histidine), and [4Fe-4S] clusters can have ligands containing oxygen atoms (aspartic acid) or even hydroxyl or water molecules (26). Recently, the x-ray structure of *Desulfovibrio gigas* hydrogenase showed a new type of tetranuclear cluster binding with one histidine and three cysteines in the coordination sphere (27).

The presence of one oxygen atom in a biological [4Fe-4S]$^{+2}$ cluster has been studied by Mössbauer spectroscopy in substrate-free form of aconitase: the site with no sulfur coordination has a δ_{av} = 0.46 mm/s and ΔE_{Qav} = 1.20 mm/s (25).

The amino acid sequence of enoate reductase was recently determined[1] and compared with other related enzymes whose primary structures where available (29). A conserved pattern $CX_2CX_{2-3}CX_{11-13}C$ was detected. For enoate reductase, the cysteine anticipated to bind the cluster (*i.e.*, C364, C367, C371, and C384) are supported by x-ray structural data obtained on the related trimethylamine dehydrogenase (30). On the basis of this observation, the enoate reductase center should only involve cysteinyl coordination.

However, the spectral parameters here reported for oxidized enoate reductase (δ_{av} = 0.46 mm/s, and ΔE_{Qav} = 1.36 mm/s) also suggested a non-sulfur coordination at the cluster when compared with substrate-free aconitase. The coordination number, however, should not be higher than four, because a highly differentiated site is not observable. In the +1 state, all [4Fe-4S]-containing proteins characterized so far exhibit δ_{av} between 0.52 and 0.59 mm/s (hydrogenases have smaller reported values of 0.47/0.49) and ΔE_Q between 1.15 and 1.75 mm/s (19, 31–33, 35–39).

The work performed in reduced aconitase bound to citrate and other substrates has shown a specific iron (Fe_a), which has penta/octahedral coordination, which results in a value of +2.5 mm/s for ΔE_Q and 0.99 mm/s of isomer shift, whereas its tetrahedral counterpart iron (Fe_{b1}) has ΔE_Q = -2.5 mm/s and δ = 0.64 mm/s (25).

[1] A. Bacher, personal communication.

Enoate reductase exhibits the highest reported average ΔE_Q (1.91 mm/s) and a δ average value (0.58 mm/s) that is much more similar to the one found in APS center I (37). These results suggest also that enoate reductase should have a different chemical environment, giving a stronger ferrous character to this cluster component. The Mössbauer studies on aconitase enable us to discard the possibility of having ferrous ions coordinated by five or six ligands; however, some distinction can be made relative to the ferredoxin type of clusters. The strong ferrous character (compared with ferredoxin $[4Fe\text{-}4S]^{1+}$ clusters) in the dithionite-reduced state corroborates the above mentioned character also found in the protein as isolated.

Mechanistic Implications of the Coordination of the Enoate Reductase [4Fe-4S] Cluster—The coordination of iron-sulfur proteins by nitrogens or oxygen ligands is well documented in Rieske centers ([2Fe-2S], 2 Cys or 2 His), aconitase ([4Fe-4S], 3 Cys, 1 H_2O, or substrate), *Pyrococus furiosus* ferredoxin ([4Fe-4S], 3 Cys, 1 Asp, or 1 H_2O) and recently the monohistidine coordinated cluster found in hydrogenase (27) ([4Fe-4S], 3 Cys or 1 His). Unfortunately, the Mössbauer studies on the these two last proteins provide little information, because in hydrogenase there is a spectral overlap with other clusters and *P. furiosus* ferredoxin has a ground state spin mixture ($S = 1/2$ and $S = 3/2$).

The Mössbauer parameters determined for the [4Fe-4S] cluster of enoate reductase are closely related to the substrate-free aconitase but distinct from the four cysteinyl ligation [4Fe-4S] clusters. This could be an indication of non-cysteinyl coordination at one iron site. Other plausible biological ligands can only be oxygen or nitrogen. The possibility of the direct coordination of nitrogen to the cluster was discarded by ESEEM and ENDOR studies,[2] leaving the possibility of oxygen coordination. These techniques also exclude the possibility of water or hydroxyl coordination, because the magnitudes of the observed ^1H hyperfine coupling constants are much smaller than those observed in *P. furiosus* ferredoxin and do not show any significant isotopic (H_2O/D_2O) effect.

The sequence data together with the x-ray analysis of a related protein strongly suggest that a sufficient number of cysteines are available to coordinate the metal center. We suggest that the unusual properties of the core are due to structural constrains that impose a particular electronic delocalization (ferrous character of subsites a and b) rather than non-sulfur coordination at these subsites.

Kinetic studies proposed that enoate reductase has Bi Bi Ping Pong type mechanism (7). In the first cycle the reducing agent (either NADH or reduced methyl viologen) will reduce the enzyme, making it competent to reduce the substrate (enoate or enal) double bond. Hydride transfer from NADH was proven by isotopic labeling to be stereospecific relative to the R hydrogen atom (7). The hydride transfer from NADH presumably involves the flavin cofactor.

The reduction of enoates with a halogen substituent at the β position lead to a interesting result, that the first reducing equivalents were used not to reduce the double bond but to eliminate HX from the enoate. Sedlmaier *et al.* (41) interpreted these results by proposing that a positive charge close to the carboxylate group will polarize the double bond in a way that favors the elimination reaction.

Based on the information from the Mössbauer data and the previous kinetic studies, we propose that the iron-sulfur center plays a role in the polarization of the substrate double bond, probably through second sphere coordination of the substrate carboxylate group to the cluster. This idea is supported by theoretical studies of the enzymatic reactions, where the need for a strong polarizing agent is indicated (28, 40, 42). The strongly polarized double bond is then in a favorable condition for the hydride nucleophilic attack, completing the double bond reduction.

[2] G. Daeges, J. Caldeira, H. White, R. Feicht, J. J. G. Moura, H. Simon, I. Moura, and J. Huttermann, submitted for publication.

REFERENCES

1. Tischer, W., Bader, J., and Simon, H. (1979) *Eur. J. Biochem.* **97,** 103–112
2. Giesel, H., and Simon, H. (1983) *Arch. Microbiol.* **135,** 51–57
3. Simon, H. (1991) in *Chemistry and Biochemistry of Flavoenzimes* (Müller, F., ed) Vol. II, pp. 317–328, CRC Press, Boca Raton, FL
4. Simon, H., Bader, J., Giinther, H., Neumann, S., and Thanos, J. (1985) *Angew. Chem. Int. Ed. Engl.* **24,** 539–553
5. Bühler, M. (1981) Untersuchungen zu Substrat-spezifität, Kinetic und Mechanismus von Enoat-Reduktasen aus Clostridien Ph.D. thesis, Technischen Universität, Munich, Germany
6. Bader, J., and Simon, H. (1983) *FEMS Microbiol. Lett.* **20,** 171–175
7. Bühler, M., and Simon, H. (1982) *Hoppe-Seyler's Z. Physiol. Chem.* **363,** 609–625
8. Thanos, I., Deffner, A., and Simon, H. (1988) *Biol. Chem. Hoppe-Seyler* **369,** 451–460
9. Kuno, S., Bacher, A., and Simon, H. (1985) *Biol. Chem. Hoppe-Seyler* **366,** 463–472
10. Cammack, R. (1992) in *Advances in Inorganic Chemistry - Iron Sulfur Proteins* (Sykes, A. G., and Cammack, R., eds) Vol. 38, pp. 281–322, Academic Press, Inc.
11. Emptage, M. H. (1988) in *Metal Clusters in Proteins*, pp. 343–371, American Chemical Society, Washington, D. C.
12. Beinert, H., and Kennedy, M. C. (1989) *Eur. J. Biochem.* **186,** 5–15
13. Switzer, R. L. (1989) *Biofactors* **2,** 77–86
14. Cunningham, R. P., Asahara, H., Bank, J. F., Scholes, C. P., Salerno, J. C., Surerus, K., Münck, E., McCracken, J., Peisach, J., and Emptage, M. H. (1989) *Biochemistry* **28,** 4450–4455
15. Cox, T. C., Bawden, M. J., Martin, A., and May, B. K. (1991) *EMBO J.* **10,** 1891–1896
16. Rouault, T. A., Stout, C. D., Kaptain, S., Harford, J. B., and Klausner, R. D. (1991) *Cell* **64,** 881–883
17. Robbins, A. H., and Stout, C. D. (1989) *Proc. Natl. Acad. Sci. U. S. A.* **86,** 3639–3641
18. Dutton, P. L. (1971) *Biochim. Biophys. Acta* **226,** 63–80
19. Teixeira, M., Moura, I., Xavier, A. V., Moura, J. J. G., Le Gall, J., Der Vartanian, D. V., Peck, H. D., Jr., and Huynh, B. H. (1989) *J. Biol. Chem.* **264,** 16435–16450
20. Caldeira, J., Palma, N., Lampreia, J., Regalla, M., Calvete, J., Schafer, W., Moura, I., LeGall, J., and Moura, J. J. G (1994) *Eur. J. Biochem.* **220,** 987–995
21. Palmer, G., Müller, F., and Massey, V. (1971) in *Flavins and Flavoproteins* (Kamin, H., ed) pp. 123–137, University Park Press, Baltimore
22. Christner, J. A., Janick, P. A., Siegel, L. M., and Münck, E. (1983) *J. Biol. Chem.* **258,** 11157–11164
23. Kent, T. A., Dreyer, J.-L., Kennedy, M. C., Huynh, B. H., Emptage, M. H., Beinert, H., and Münck, E. (1982) *Proc. Natl. Acad. Sci. U. S. A.* **79,** 1096–1100
24. Kent, T. A., Emptage, M. H., Merkle, H., Kennedy, M. C., Beinert, H., and Münck, E. (1985) *J. Biol. Chem.* **260,** 6871–6881
25. Emptage, M. H., Kent, T. A., Kennedy, M. C., Beinert, H., and Münck, E. (1983) *Proc. Natl. Acad. Sci. U. S. A.* **80,** 4674–4678
26. Moura, J. J. G., Macedo, A. L., and Palma, P. N. (1994) in *Methods in Enzymology, Inorganic Microbial Sulfur Metabolism* (Peck, H. D., Jr., and LeGall, J., eds) Vol. 243, pp. 165–188, Academic Press, New York
27. Volbeda, A., Charon, M.-H., Piras, C., Hatchikian, E. C., Frey, M., and Fantecilla-Camps, J. C. (1995) *Nature* **373,** 580–587
28. Flint, D. H., Emptage, M. H., Finnegan, M. G., Fu, W., and Johnson, M. K. (1993) *J. Biol. Chem.* **268,** 14732–14742
29. Franklund, C. V., Baron, S. F., and Hylemon, P. B. (1993) *J. Bacteriol* **175,** 3002–3012
30. Barber, M. J., Neame, P. J., Lim, L. W., White, S., and Mathws, F. S. (1992) *J. Biol. Chem.* **267,** 6611–6619
31. Moura, J. J. G., Moura, I., Kent, T. A., Lipscomb, J. D., Huynh, B. H., LeGall, J., Xavier, A. V., and Münck, E. (1982) *J. Biol. Chem.* **257,** 6259–6267
32. Middelton, P., Dickson, D. P. E., Jonhson, C. E., and Rush, J. D. (1978) *Eur. J. Biochem.* **88,** 135–141
33. Geary, P. J., and Dickson, D. P. E. (1981) *Biochem. J.* **195,** 199–203
34. Deleted in proof
35. Teixeira, M., Moura, I., Fauque, G., DerVartanian, D. V., LeGall, J., Peck, H. D., Jr., Moura, J. J. G., and Huynh, B. H. (1990) *Eur. J. Biochem.* **189,** 381–386
36. Moura, I., LeGall, J., Lino, A. R., Peck, H. D., Jr., Fauque, G., Xavier, A. V., DerVartanian, D. V., Moura, J. J. G., and Huynh, B. H. (1990) *J. Am. Chem. Soc.* **110,** 1075–1082
37. Lampreia, J., Moura, I., Teixeira, M., Peck, H. D., Jr., LeGall, J., Huynh, B. H., and Moura, J. J. G. (1990) *Eur. J. Biochem.* **188,** 653–664
38. Middelton, P., Dickson, P. E. D., Johnson, C. E., and Rush, J. D. (1980) *Eur. J. Biochem.* **104,** 289–296
39. Kent, T. A., Emptage, M. H., Merkle, H., Kennedy, M. C., Beinert, H., and Münck, E. (1985) *J. Biol. Chem.* **260,** 6871–6881
40. Gerlt, J. A., and Gassman, P. G. (1992) *J. Am. Chem. Soc.* **114,** 5929–5934
41. Sedlmaier, H., Tischer, W., Rauschenbach, P., and Simon, H. (1979) *FEBS Lett.* **100,** 129–132
42. Scherf, U., and Buckel, W. (1993) *Eur. J. Biochem.* **215,** 421–429

EPR and Mössbauer Spectroscopic Studies on Enoate Reductase

Jorge Caldeira, Richard Feicht, Hiltturd White, Miguel Teixeira, José J. G. Moura, Helmut Simon and Isabel Moura

J. Biol. Chem. 1996, 271:18743-18748.
doi: 10.1074/jbc.271.31.18743